Manufacture and evaluation of nano-silver-poly-DL-lactide-co-caprolactone-small intestinal submucosa biological mesh in abdominal wall reconstruction

Li Zhu[1#], Hui Li[2#], Yizhu Chen[1], Yongjing Dai[1], Xiru Li[1]

[1]Senior Department of General Surgery, The First Medical Center of PLA General Hospital, Beijing, China; [2]Senior Department of Vascular Surgery, The First Medical Center of PLA General Hospital, Beijing, China

Contributions: (I) Conception and design: X Li, Y Dai, L Zhu; (II) Administrative support: X Li, Y Dai; (III) Provision of study materials or patients: L Zhu, H Li, Y Chen; (IV) Collection and assembly of data: L Zhu, H Li; (V) Data analysis and interpretation: L Zhu, H Li; (VI) Manuscript writing: All authors; (VII) Final approval of manuscript: All authors.

[#]These authors contributed equally to this as co-first authors.

Correspondence to: Xiru Li, MD. Senior Department of General Surgery, The First Medical Center of PLA General Hospital, 28 Fuxing Road, Haidian District, Beijing 100853, China. Email: 2468li@sina.com.

Background: Inguinal hernia repair is a routine surgical procedure and many methods are being applied to improve the operation. In this study, an abdominal wall defect model was established in New Zealand rabbits. The safety and efficacy of the test product was evaluated by observing the physiological state and clinical manifestations and conducting anatomical observations in the rabbits after use of the nano-silver-poly-DL-lactide-co-caprolactone-small intestinal submucosa (NS-PLCL-SIS) mesh.

Methods: A total of 18 New Zealand rabbits were randomly divided into a test group and a blank group. Routine blood and serum biochemical tests, and anatomical observations were conducted on postoperative day 30 (D30), day 60 (D60), and day 90 (D90). During the study period, all animals underwent clinical observation, and the obtained data were counted.

Results: The results showed that the NS-PLCL-SIS mesh was degraded within 90 days, and there was no abnormal reaction and no animal death during the test. There was no significant difference in the changes of animal body weight at each time point. There was no infectious inflammatory reaction in the wound at the study site, and the ocular wound healed well 7 days after the operation.

Conclusions: Under the conditions of this experiment, the NS-PLCL-SIS mesh had good performance in the repair of abdominal wall defect in New Zealand rabbits and is clinically safe for veterinarians.

Keywords: Porcine small intestinal submucosal tissue; biological mesh; regeneration; abdominal wall

Submitted Dec 23, 2022. Accepted for publication Jul 19, 2023. Published online Oct 27, 2023.
doi: 10.21037/atm-22-6538
View this article at: https://dx.doi.org/10.21037/atm-22-6538

Introduction

In general surgery, inguinal hernia repair is one of the most routine operations worldwide (1). With the advancement of science and technology, it has become a complex procedure with many methods being applied to improve the surgery and reduce the risk of complications. Porcine small intestinal submucosa (P-SIS) is a novel bioactive material with major SIS components including proteoglycans, glycosaminoglycans, glycoproteins, and growth factors (2). Compared with other synthetic materials, P-SIS is easy to handle and does not elicit an immune response in the recipient organism (3). P-SIS has good compatibility with smooth muscle cells as well as endothelial and neural cells, and it can be used as a safety material. To date, P-SIS has been successfully implemented as biological meshes in

clinical practice (4). However, clinical practice has revealed that normal biological meshes have limitations such as poor mechanical properties, and become very soft after hydration, making them especially inconvenient to operate under laparoscopy; such issues prolong the operation time and increase the difficulty of the operation (5).

The unique properties of nanosilver (NS), such as antimicrobial activity and biocompatibility, make it an attractive material for use in medical devices and implants. NS has been shown to effectively kill bacteria and prevent infection, making it particularly useful in wound healing and in preventing implant-associated infections (6). Additionally, NS has been found to have anti-inflammatory and immunomodulatory effects, which may have therapeutic potential in a range of diseases (7).

Poly-DL-lactide-co-caprolactone (PLCL) is a biodegradable and biocompatible polymer, which is a very flexible and rubber-like elastic copolymer (8). Accordingly, PLCL has many potential uses in relation to soft tissue regeneration (9), such as in blood vessels, tendons, skin, esophagus, and cardiac tissues (10).

In this study, a new hybrid mesh nano-silver-poly-DL-lactide-co-caprolactone-small intestinal submucosa (NS-PLCL-SIS) was synthesized by using NS, PLCL, and P-SIS. New Zealand rabbits were used as a model to evaluate the safety and efficacy of the NS-PLCL-SIS biological mesh by observing the physiological state, clinical manifestations, and anatomical observations of the trauma model animals after using the NS-PLCL-SIS biological mesh. We present this article in accordance with the ARRIVE reporting checklist (available at https://atm.amegroups.com/article/view/10.21037/atm-22-6538/rc).

Highlight box

Key findings

- We manufactured a new nano-silver-poly-DL-lactide-co-caprolactone-small intestinal submucosa (NS-PLCL-SIS) biological mesh for abdominal wall reconstruction, and evaluated the performance in New Zealand rabbits.

What is known and what is new?

- Mesh is needed for abdominal wall reconstruction. Currently, biological mesh is widely used because of its good biocompatibility.
- Pure biological mesh often faces the problem of insufficient mechanical properties, and synthetic mesh is the trend.

What is the implication, and what should change now?

- Our findings indicate that NS-PLCL-SIS biological mesh may have the potential to reduce the occurrence and recurrence of hernia in the future.

Methods

Ethical statement

Experiments were performed under a project license (No. 20160010703) granted by Animal Research Committee of PLA General Hospital. All experiments were performed according to the Guidelines for the Care and Use of Laboratory Animals in China. A protocol was prepared before the study without registration.

Animals

New Zealand rabbits were purchased from Vital River Laboratory Animal Technology (Beijing, China). The rabbits were maintained in a specific-pathogen-free (SPF) environment on a 12-hour light/dark cycle with access to food and water. The rabbits were fasted for 16 hours before surgery, then weighed, and Zoletil (0.04 mL/kg, intravenous injection) and Sumianxin Ⅱ (0.06 mL/kg, intramuscular injection) were used for combined anesthesia. The rabbits were placed on the operating table in a supine position, and the supine limbs were secured. Blood was collected from the ear margin for the determination of blood count and serum biochemistry. The skin of the rabbit's abdomen was exposed and then sterilized with active iodine. A sterile surgical list was lain out and the surgical area was exposed. An incision of about 5 cm in length was made, followed by blunt separation of subcutaneous tissue and muscles and exposure of abdominal wall, and the creation of 2 cm defects, to establish a New Zealand rabbit abdominal wall defect model. Then, 2.5 cm × 2.5 cm hernia mesh was implanted into the abdominal wall, sutured, and fixed around the perimeter, with the end of the layer finally closed. After the operation, 20 IU/kg of penicillin sodium (North China Pharmaceutical Group Corp., Shijiazhuang, China) with 0.9% normal saline was administered via intramuscular injection twice a day to prevent infection. The investigators then conducted intensive care, detailed observation of clinical changes, and documentation. Daily combination treatment was continually administered to prevent infection. The 18 rabbits were dissected at the planned time points [postoperative day 30 (D30), D60, and D90] to observe the repair of abdominal wall defects, whether there was an

Table 1 The detection of meshes thickness, breaking force, bending length

Test item	Mean ± SD
Length (mm)	10.00±0.00
Width (mm)	7.00±0.00
Thickness (mm)	0.56±0.00
Breaking force (N)	31.78±0.18
Bending length (mN/cm)	7.22±0.08

SD, standard deviation.

inflammatory reaction, and whether there was any residue of the test products.

Manufacture of NS-PLCL-SIS meshes

Based on the relatively mature Abraham method, the submucosal tissue of the porcine small intestine was decellularized and the fat, endotoxin, cytotoxicity, growth factors, and biomechanics in the P-SIS material were detected to understand the basic information of P-SIS material. The NS was attached to the P-SIS and cross-woven into a surface with the PLCL elastomeric fiber, and secured by hydration paste, followed by uninterrupted vacuum lamination 24 hours after disinfection preservation.

Detection of mesh thickness

After lyophilization, 5 pieces of each NS-PLCL-SIS mesh were randomly selected, and a thickness detector (Shanghai Precision & Scientific Instrument Co., Ltd., Shanghai, China) was used to detect the thickness of each sample.

Detection of the mesh breaking force

The maximum tensile strength of the sample was detected by the uniaxial tensile failure test with the electronic detector. P-SIS tissue was hydrated in water for 4 minutes prior to testing. The sample was continuously stretched at 10 cm/minute, and the change of tension value was observed. When the tension suddenly dropped at the peak, the tension value was recorded, and the breaking force of the sample was calculated with a pharmaceutical packaging performance tester (Labthink Electromechanical Technology Co., Ltd., Jinan, China).

Detection of mesh bending length

According to the standard of GB/T18318.1-2009, the bending length of the sample was tested by the inclined plane method. The rectangular pattern was placed on the horizontal platform, the long axis of the pattern was held parallel to the long axis of the platform, and the pattern was pushed along the long axis to make it extend out of the platform and bend under the dead weight. The protruding part ended in the air, and a ruler was used to hold down the other part still on the platform. When the head end of the pattern passed through the leading edge of the platform to reach an inclined plane at an angle of 41.5° from the horizontal line, the length of the protruding part was deemed equal to twice the bending length of the pattern and the bending length could be calculated. After freeze-drying, 5 pieces of each NS-PDO-SIS mesh were randomly selected and trimmed to the size of 25 mm × 160 mm. The NS-PDO-SIS mesh was hydrated in normal saline for 10 minutes before the test. The bending length was investigated with an electronic hardness tester (Dayuan Electronic Instruments Co., Ltd., Lanzhou, China).

Statistical analysis

Data analysis was performed using GraphPad Prism (version 8.1 for Windows; GraphPad Software, San Diego, CA, USA). Levels of statistical significance for all data were determined by two-way analysis of variance (ANOVA). The results were expressed as mean and standard deviation (means ± standard deviation).

Results

Physical performance test of NS-PLCL-SIS mesh

After making the NS-PLCL-SIS mesh, 5 mesh samples were randomly selected to test the physical properties. The thickness, breaking force, and bending length of NS-PLCL-SIS mesh were tested. The results showed that the average thickness of the meshes was 0.555 mm, the average breaking force of the meshes was 31.779 N, and the average bending length of the meshes was 7.223 mN/cm (see *Table 1*).

Clinical detection index

The rabbits' behavioral activity, mental condition, appetite,

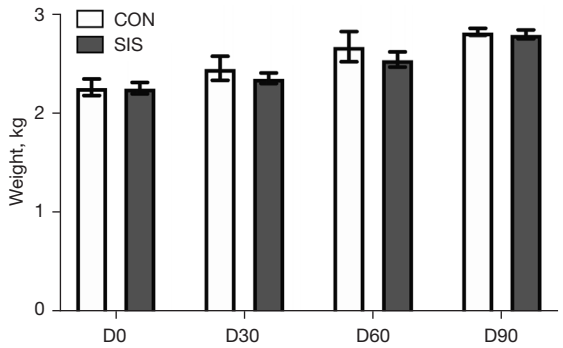

Figure 1 Body weight of rabbits on D0, D30, D60, and D90 after surgery. CON, control group; SIS, NS-PLCL-SIS group; NS-PLCL-SIS, nano-silver-poly-DL-lactide-co-caprolactone-small intestinal submucosa; D0, day 0; D30, day 30; D60, day 60; D90, day 90.

and food intake returned to normal 3 days after surgery, the animals safely passed the perioperative period, and there was no significant change in the appearance and signs such as urinary traits, glandular secretion, and body weight before and after the operation. All 18 animals had no significant change in weight between control group (CON) and NS-PDO-SIS group (SIS) during postoperative D0, D30, D60, and D90 (*Figure 1*).

Routine blood and blood biochemistry detection

In this study, blood routine and blood biochemical tests were performed on D0, D30, D60, and D90. The results showed that after the use of NS-PLCL-SIS biological mesh, no abnormal reactions were found in the observation of serum biochemical indexes, each value was within the clinical reasonable range of veterinarians, there were no symptoms of immune rejection reaction, and the hematologic indicators showed that the individual health of each animal was good (*Figures 2-7*).

Evaluation of adhesion between mesh and tissue

The intraperitoneal adhesions of 18 rabbits were observed at D30, D60, and D90, and the degree of adhesions was scored according to the scoring standards in the guidelines for the technical review of mesh animal experiments (see *Table 2*). The score results showed that there was no significant difference in extent of adhesions and area of adhesions between SIS group and CON group at D30, D60, and D90 (*Figure 8A*).

Anatomical observations

The rabbits were anatomically observed at different time points after surgery. No infection in the operating area was seen, and there was no significant change in the shape, color, and size of other organs after surgery. At D30, the wound was not completely healed, and the residue of the mesh could be observed with the naked eye. There was no adhesion between the CON group and the SIS group. A small amount of pus could be seen in the wound and abdominal wall. At D60, the wound was completely healed, no meshes were visible, no adhesions were seen in the CON group and SIS group, and no abscesses and pus were seen in the wound and abdominal wall. At D90, the wound was completely healed, no meshes were visible, no adhesions were seen in the CON group and SIS group, and no abscesses and pus were seen in the wound and abdominal wall (*Figure 8B*).

Discussion

A variety of extracellular matrix (ECM) materials have been used in the field of regenerative medicine and reconstructive medicine (11). ECM materials have a unique three-dimensional (3D) spatial structure and contain a large number of bioactive factors, including collagen, glucosaminoglycan, and growth factors, which can induce the migration and differentiation of host cells after implantation *in vivo* (12). Research confirms that the use of an ECM mesh may be appropriate in cases with very thin dermis that are particularly prone to flattening or in revision cases where the first procedure has already failed (13). Compared with synthetic mesh, ECM biological mesh has high biological activity, but its mechanical properties are relatively insufficient, which cannot meet the diversified needs in clinical practice. Therefore, it is of great clinical significance to improve the mechanical properties of biological mesh. Some researchers have used ECM and artificial materials to produce hybrid mesh, which has better mechanical properties than pure ECM mesh (14), but may cause the loss of bioactive factors and damage the 3D structure of ECM in the process of gel production.

P-SIS is an acellular biological ECM that has been

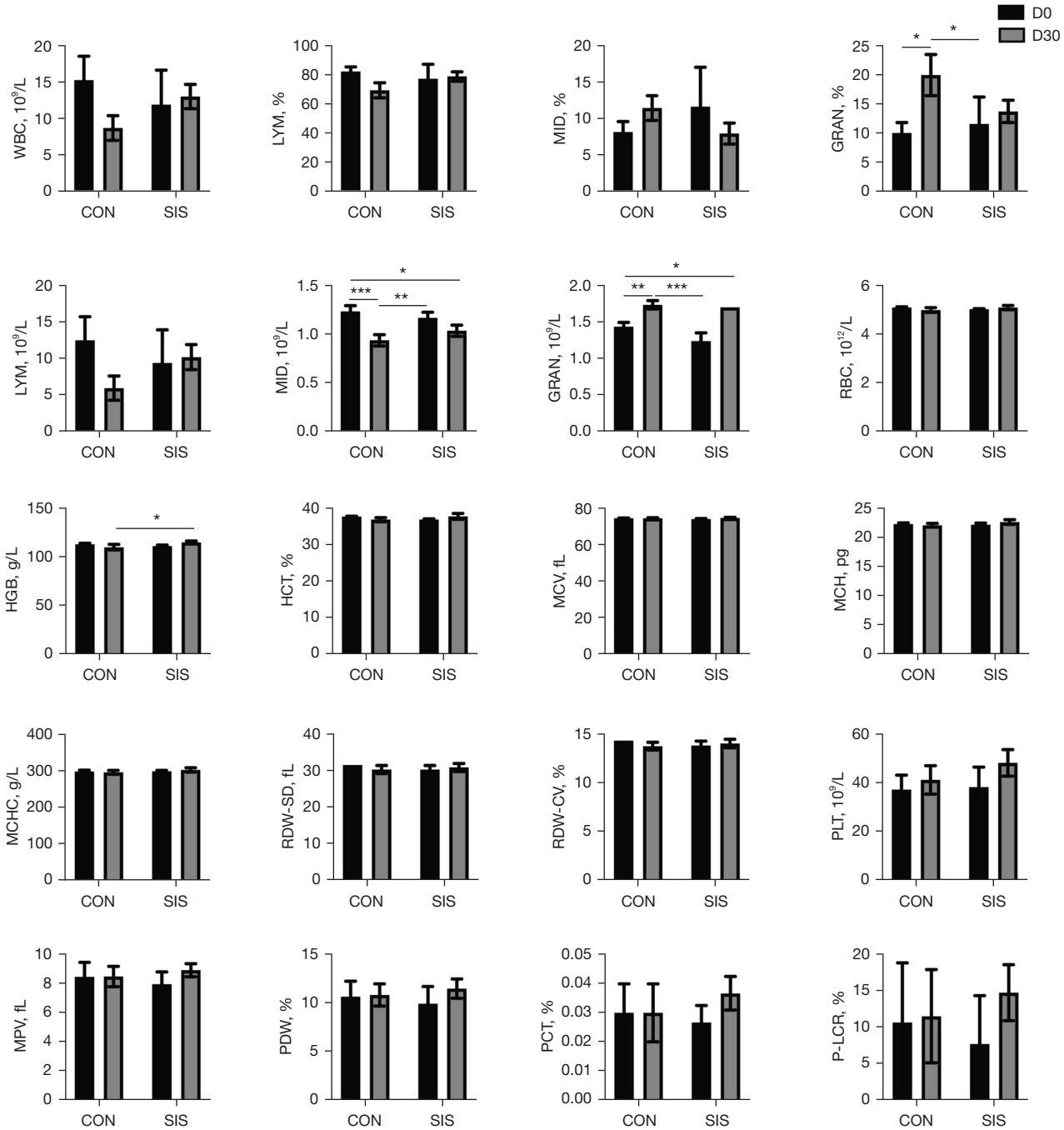

Figure 2 Blood routine indicators of rabbits at D0 and D30. Levels of statistical significance for all data were determined by two-way analysis of variance (*, P<0.05; **, P<0.01; ***, P<0.001, indicates significant difference between the two groups). CON, control group; SIS, NS-PLCL-SIS group; NS-PLCL-SIS, nano-silver-poly-DL-lactide-co-caprolactone-small intestinal submucosa; D0, day 0; D30, day 30; WBC, white blood cell; LYM, lymphocyte; MID, intermediate cell; GRAN, granulocyte; RBC, red blood cell; HGB, hemoglobin; HCT, hematocrit; MCV, mean corpuscular volume; MCH, mean corpuscular hemoglobin; MCHC, mean corpuscular hemoglobin concentration; RDW-SD, standard deviation from the red blood cell volume distribution width; RDW-CV, coefficient of variation from the red blood cell volume distribution width; PLT, platelet count; MPV, mean platelet volume; PDW, platelet distribution width; PCT, plateletocrit; P-LCR, proportion of large platelets.

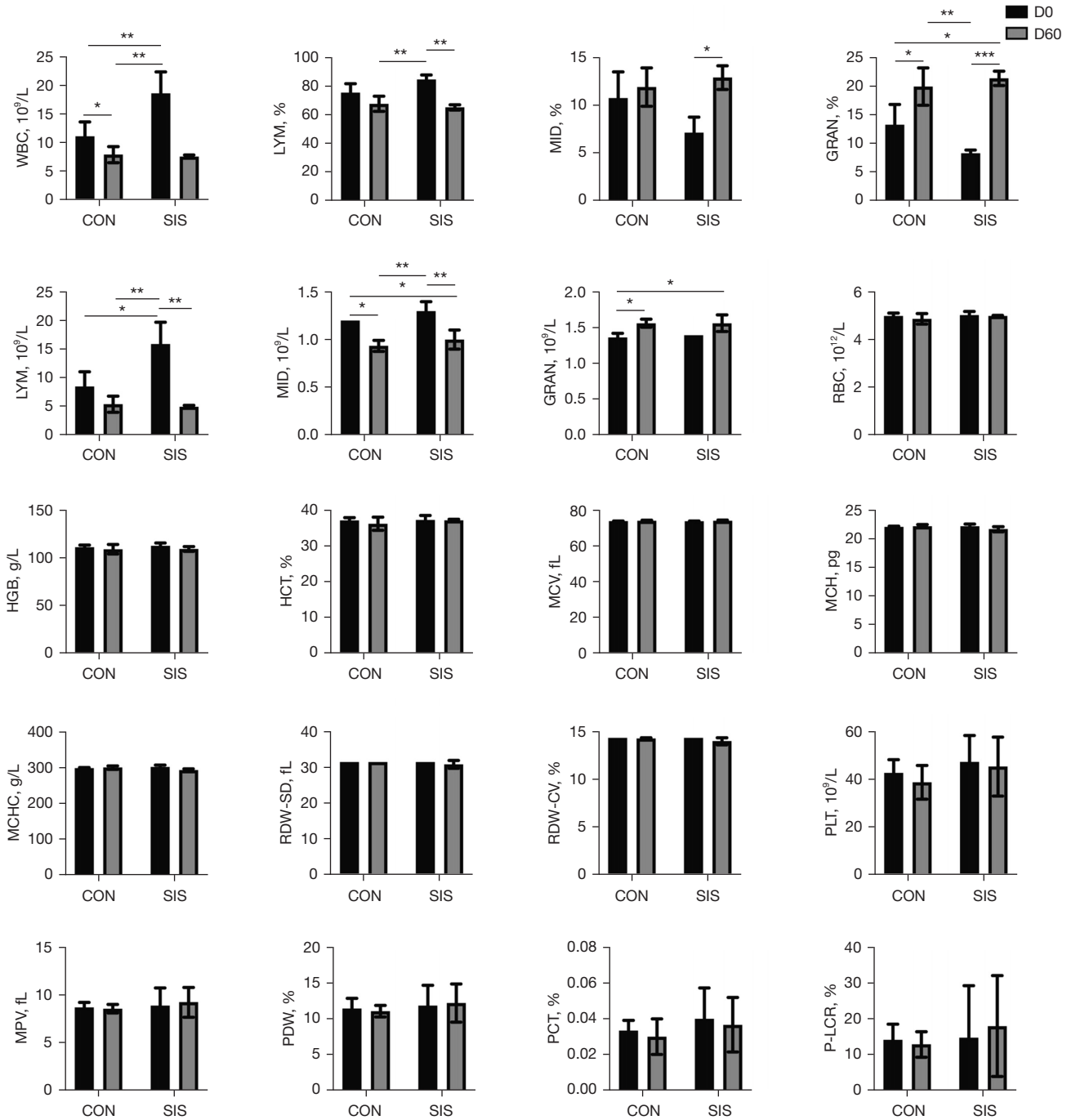

Figure 3 Blood routine indicators of rabbits at D0 and D60. Levels of statistical significance for all data were determined by two-way analysis of variance (*, P<0.05; **, P<0.01; ***, P<0.001, indicates significant difference between the two groups). CON, control group; SIS, NS-PLCL-SIS group; NS-PLCL-SIS, nano-silver-poly-DL-lactide-co-caprolactone-small intestinal submucosa; D0, day 0; D60, day 60; WBC, white blood cell; LYM, lymphocyte; MID, intermediate cell; GRAN, granulocyte; RBC, red blood cell; HGB, hemoglobin; HCT, hematocrit; MCV, mean corpuscular volume; MCH, mean corpuscular hemoglobin; MCHC, mean corpuscular hemoglobin concentration; RDW-SD, standard deviation from the red blood cell volume distribution width; RDW-CV, coefficient of variation from the red blood cell volume distribution width; PLT, platelet count; MPV, mean platelet volume; PDW, platelet distribution width; PCT, plateletocrit; P-LCR, proportion of large platelets.

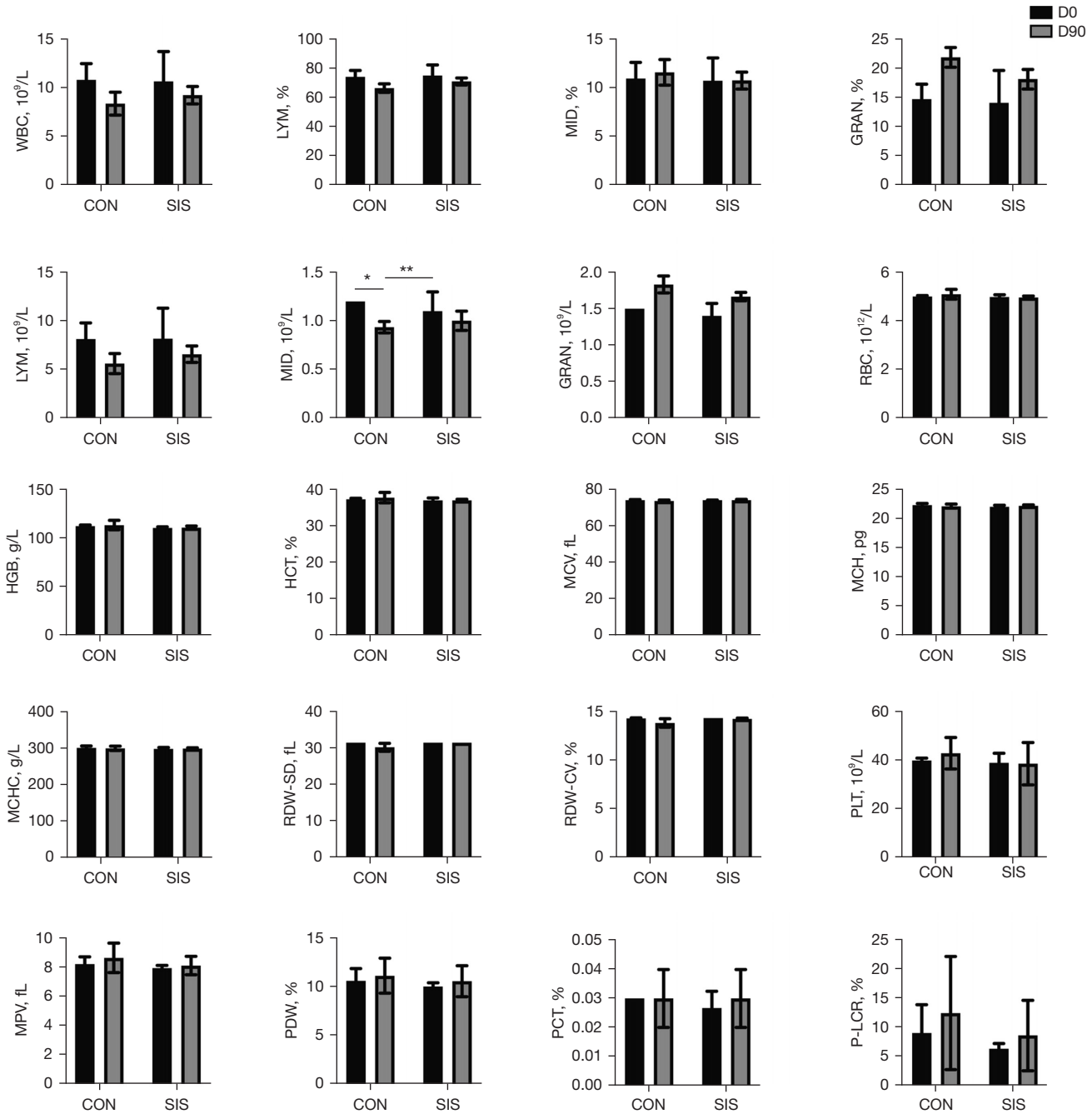

Figure 4 Blood routine indicators of rabbits at D0 and D90. Levels of statistical significance for all data were determined by two-way analysis of variance (*, P<0.05; **, P<0.01, indicates significant difference between the two groups). CON, control group; SIS, NS-PLCL-SIS group; NS-PLCL-SIS, nano-silver-poly-DL-lactide-co-caprolactone-small intestinal submucosa; D0, day 0; D90, day 90; WBC, white blood cell; LYM, lymphocyte; MID, intermediate cell; GRAN, granulocyte; RBC, red blood cell; HGB, hemoglobin; HCT, hematocrit; MCV, mean corpuscular volume; MCH, mean corpuscular hemoglobin; MCHC, mean corpuscular hemoglobin concentration; RDW-SD, standard deviation from the red blood cell volume distribution width; RDW-CV, coefficient of variation from the red blood cell volume distribution width; PLT, platelet count; MPV, mean platelet volume; PDW, platelet distribution width; PCT, plateletocrit; P-LCR, proportion of large platelets.

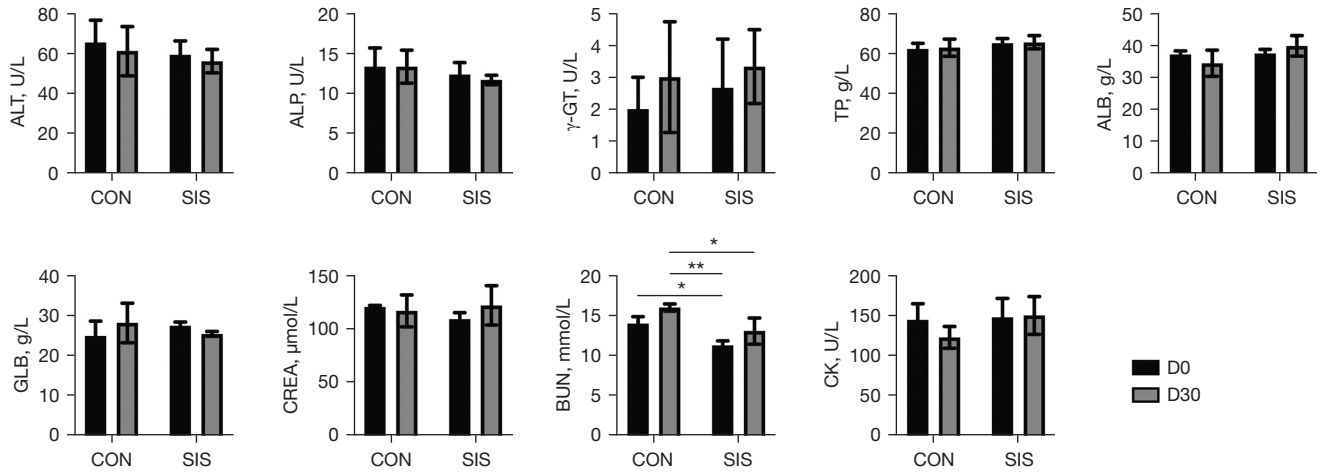

Figure 5 Blood biochemical indicators of rabbits at D0 and D30. Levels of statistical significance for all data were determined by two-way analysis of variance (*, P<0.05; **, P<0.01, indicates significant difference between the two groups). CON, control group; SIS, NS-PLCL-SIS group; NS-PLCL-SIS, nano-silver-poly-DL-lactide-co-caprolactone-small intestinal submucosa; D0, day 0; D30, day 30; ALT, alanine aminotransferase; ALP, alkaline phosphatase; γ-GT, γ-glutamyl transpeptidase; TP, total protein; ALB, albumin; GLB, globulin; CREA, creatinine; BUN, blood urea nitrogen; CK, creatine kinase.

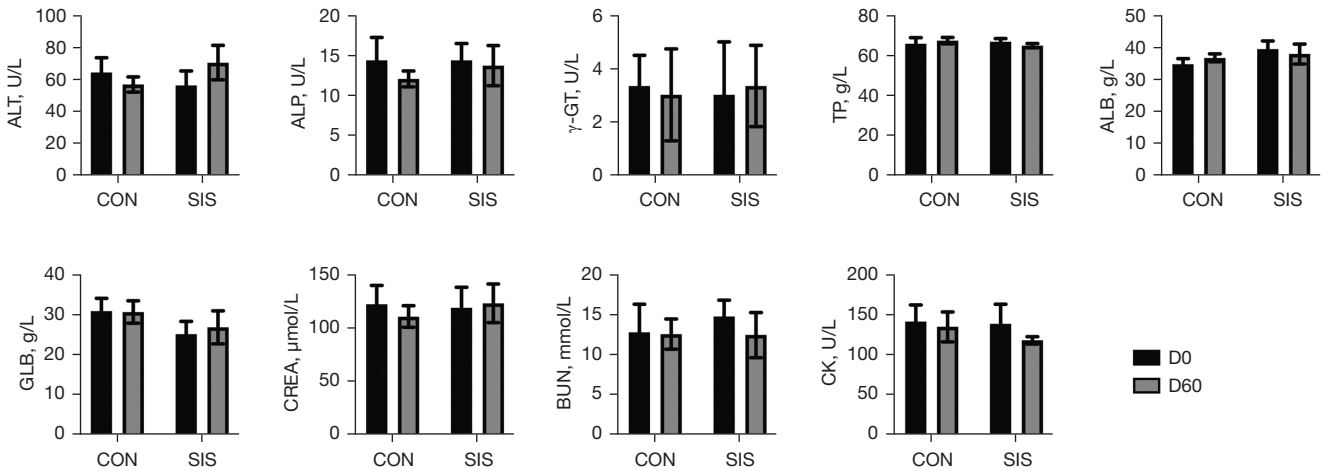

Figure 6 Blood biochemical indicators of rabbits at D0 and D60. CON, control group; SIS, NS-PLCL-SIS group; NS-PLCL-SIS, nano-silver-poly-DL-lactide-co-caprolactone-small intestinal submucosa; D0, day 0; D60, day 60; ALT, alanine aminotransferase; ALP, alkaline phosphatase; γ-GT, γ-glutamyl transpeptidase; TP, total protein; ALB, albumin; GLB, globulin; CREA, creatinine; BUN, blood urea nitrogen; CK, creatine kinase.

found to significantly improve the healing of difficult-to-heal or chronic wounds in humans. Similar to dermal ECM, SIS contains collagen, elastin, glycosaminoglycans, proteoglycans, and growth factors that play important roles in healing (15). In this experiment, PLCL-SIS biological mesh was successfully synthesized by vacuum lamination combining sheet P-SIS with PLCL. Compared with other traditional mesh, PLCL-SIS mesh has stronger shape memory characteristics and excellent mechanical properties, giving it a better handling feel in clinical use. In addition, repeated topical application of NS was reported to reduce skin inflammation (16). Due to the good antibacterial and anti-inflammatory effects of NS, this study combined PLCL-SIS and NS to synthesize NS-PLCL-SIS biological

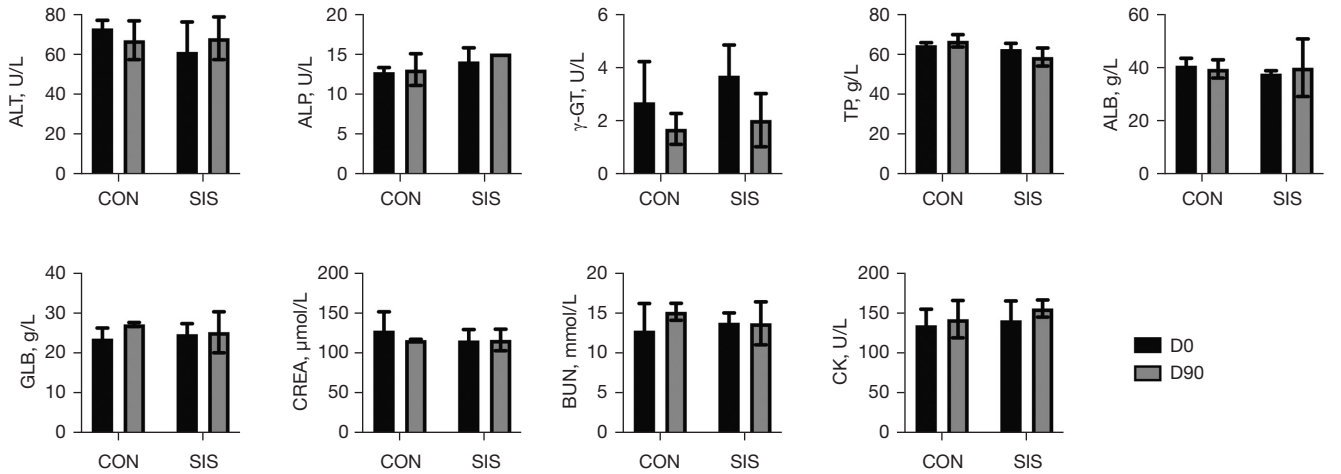

Figure 7 Blood biochemical indicators of rabbits at D0 and D90. CON, control group; SIS, NS-PLCL-SIS group; NS-PLCL-SIS, nano-silver-poly-DL-lactide-co-caprolactone-small intestinal submucosa; D0, day 0; D90, day 90; ALT, alanine aminotransferase; ALP, alkaline phosphatase; γ-GT, γ-glutamyl transpeptidase; TP, total protein; ALB, albumin; GLB, globulin; CREA, creatinine; BUN, blood urea nitrogen; CK, creatine kinase.

Table 2 Evaluation of adhesion between mesh and abdominal tissues and organs

Score	Adhesion degree	Adhesion area
0	No adhesion	No adhesion
1	One to two slight adhesions, which are pulled open as soon as they are pulled	Less than 25% of the total contact area between the mesh and the tissue
2	More than two adhesions, can be separated with no trace after separation	25–49% of the total contact area between the mesh and the tissue
3	Multiple adhesions, difficult to separate	50–74% of the total contact area between the mesh and the tissue
4	Adhesion into clumps requires sharp instrumentation separation	More than 75% of the total contact area between the mesh and the tissue

mesh to meet the diversified needs in clinical practice.

In this experiment, we synthesized NS-PLCL-SIS biological mesh. Then, the New Zealand rabbits abdominal wall defect model was established, and the meshes were implanted into the abdominal wall. We found that on D30, D60, and D90 of NS-PLCL-SIS biological mesh insertion, there was no significant difference in body weight between the SIS group and CON group. This result illustrates that the NS-PLCL-SIS biological mesh did not affect the weight and behavior of New Zealand rabbits. It has been reported that in some mesh materials, such as expanded polytetrafluoroethylene (ePTFE) and polyethylene terephthalate (PET), the mesh showed signs of chronic inflammation and lack of long-term biocompatibility of synthetic materials (17). The polypropylene mesh has been shown in another study to cause deep surgical site infections (18). In our study, the blood routine of rabbits was performed. There were no significant differences in blood routine and blood biochemical indexes between the CON group and the SIS group, and all relevant indicators of routine blood tests were at normal values. These results indicated that NS-PLCL-SIS biological mesh did not cause an inflammatory reaction in the body and did not elicit significant immune responses.

Another study (19) observed that adhesion tissue implanted with mesh could manifest an intense foreign body reaction. In further continuation, we evaluated the adhesion between mesh and tissue. The results showed that NS-PLCL-SIS biological mesh did not affect the degree of tissue adhesion. Yet, another study (20) reported that

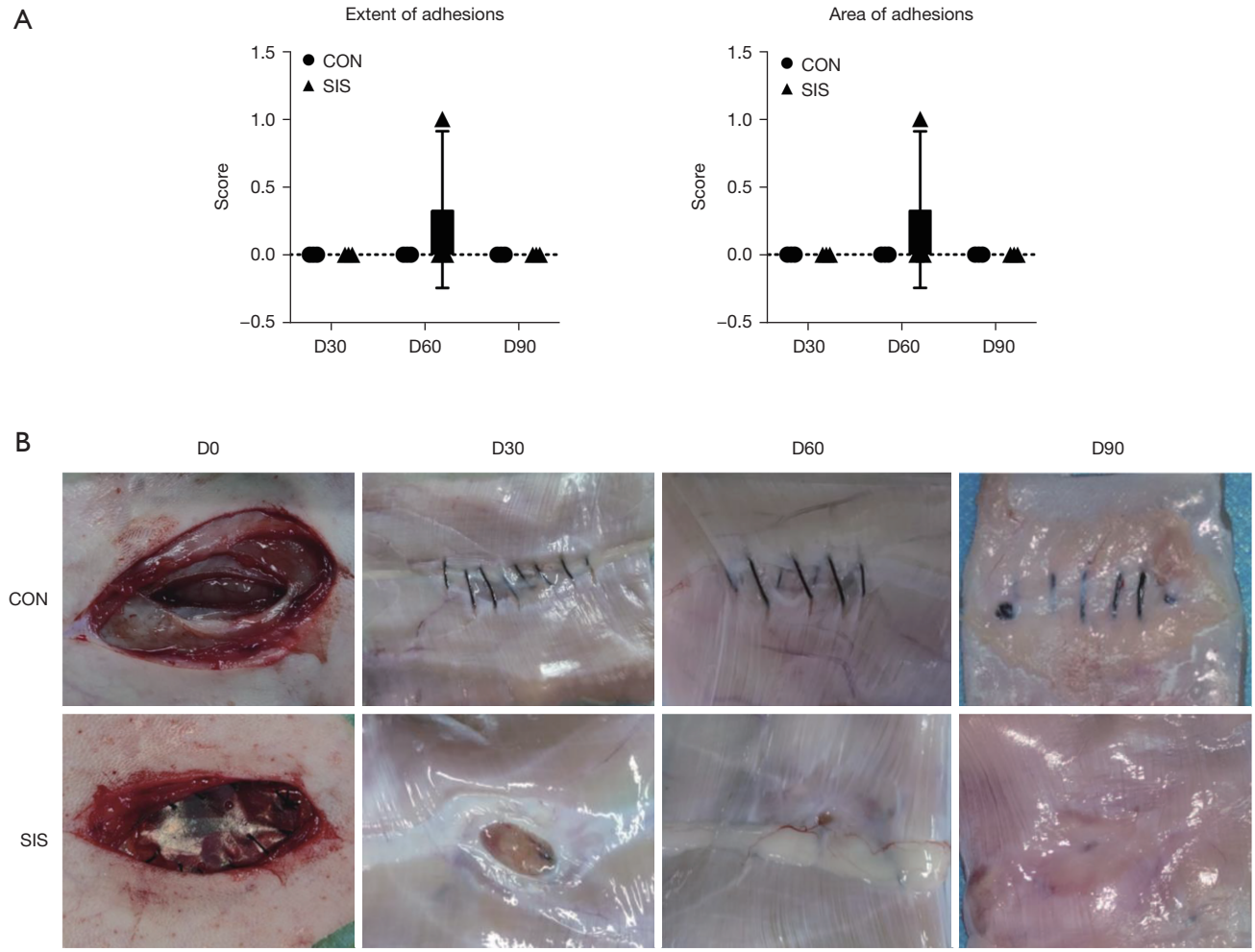

Figure 8 Evaluation of adhesion between mesh and tissue. (A) Extent of adhesions score and area of adhesions score between SIS group and CON group at D30, D60, and D90. (B) Anatomical observations of SIS group and CON group at D30, D60, and D90. CON, control group; SIS, NS-PLCL-SIS group; NS-PLCL-SIS, nano-silver-poly-DL-lactide-co-caprolactone-small intestinal submucosa; D0, day 0; D30, day 30; D60, day 60; D90, day 90.

the adverse effects of mesh implantation include delayed wound healing, early postoperative pain, and reduced trunk extension. Next, the degree of wound healing was observed, we observed the operation area at D30, D60, and D90, and found that NS-PLCL-SIS biological mesh promoted wound healing. It is suggested that NS-PLCL-SIS biological mesh has good performance in the repair of abdominal wall defect and is safe in clinical application.

Conclusions

We synthesized NS-PLCL-SIS biological mesh. Our results showed that the NS-PLCL-SIS biological mesh is safe, and it demonstrated a good reparation effect on the damaged abdominal wall. The above findings indicate that NS-PLCL-SIS biological mesh may have the potential to reduce the occurrence and recurrence of hernia in the future.

Acknowledgments

Funding: This work was funded by the Medical Science and Technology Youth Sponsorship Program (No. 20QNPY098).

Footnote

Reporting Checklist: The authors have completed the ARRIVE reporting checklist. Available at https://atm.amegroups.com/article/view/10.21037/atm-22-6538/rc

Data Sharing Statement: Available at https://atm.amegroups.com/article/view/10.21037/atm-22-6538/dss

Peer Review File: Available at https://atm.amegroups.com/article/view/10.21037/atm-22-6538/prf

Conflicts of Interest: All authors have completed the ICMJE uniform disclosure form (available at https://atm.amegroups.com/article/view/10.21037/atm-22-6538/coif). The authors have no conflicts of interest to declare.

Ethical Statement: The authors are accountable for all aspects of the work in ensuring that questions related to the accuracy or integrity of any part of the work are appropriately investigated and resolved. Experiments were performed under a project license (No. 20160010703) granted by Animal Research Committee of PLA General Hospital. All experiments were performed according to the Guidelines for the Care and Use of Laboratory Animals in China.

References

1. Birindelli A, Sartelli M, Di Saverio S, et al. 2017 update of the WSES guidelines for emergency repair of complicated abdominal wall hernias. World J Emerg Surg 2017;12:37.
2. Zhang L, Ma S, Wei P, et al. Small Intestinal Submucosa Membrane Modified by Fusion Peptide-Mediated Extracellular Vesicles to Promote Tissue Regeneration. Adv Healthc Mater 2021;10:e2101298.
3. Wang D, Ding X, Xue W, et al. A new scaffold containing small intestinal submucosa and mesenchymal stem cells improves pancreatic islet function and survival in vitro and in vivo. Int J Mol Med 2017;39:167-73.
4. Alexandridis V, Teleman P, Rudnicki M. Efficacy and safety of pelvic organ prolapse surgery with porcine small intestinal submucosa graft implantation. Eur J Obstet Gynecol Reprod Biol 2021;267:18-22.
5. Agresta F, Bedin N. Transabdominal laparoscopic inguinal hernia repair: is there a place for biological mesh? Hernia 2008;12:609-12.
6. Dong Q, Liang X, Chen F, et al. Injectable shape memory hydroxyethyl cellulose/soy protein isolate based composite sponge with antibacterial property for rapid noncompressible hemorrhage and prevention of wound infection. Int J Biol Macromol 2022;217:367-80.
7. Dong Q, Zu D, Kong L, et al. Construction of antibacterial nano-silver embedded bioactive hydrogel to repair infectious skin defects. Biomater Res 2022;26:36.
8. Jeong SI, Kim SH, Kim YH, et al. Manufacture of elastic biodegradable PLCL scaffolds for mechano-active vascular tissue engineering. J Biomater Sci Polym Ed 2004;15:645-60.
9. Liu J, Zhu H, Pei Y, et al. A methylprednisolone-loaded and core-shell nanofiber-covered stent-graft to prevent inflammation and reduce degradation in aortic dissection. Biomater Res 2022;26:15.
10. Kim D, Chung JJ, Jung Y, et al. The effect of Substance P/Heparin conjugated PLCL polymer coating of bioinert ePTFE vascular grafts on the recruitment of both ECs and SMCs for accelerated regeneration. Sci Rep 2019;9:17083.
11. Orlando G, Wood KJ, De Coppi P, et al. Regenerative medicine as applied to general surgery. Ann Surg 2012;255:867-80.
12. Divya P, Krishnan LK. Glycosaminoglycans restrained in a fibrin matrix improve ECM remodelling by endothelial cells grown for vascular tissue engineering. J Tissue Eng Regen Med 2009;3:377-88.
13. Bramhall RJ, Thiruchelvam PTR, Concepcion M, et al. Use of acellular dermal matrix (ADM) in nipple reconstruction: the 'central-pillar technique'. Gland Surg 2017;6:394-8.
14. Wolf MT, Carruthers CA, Dearth CL, et al. Polypropylene surgical mesh coated with extracellular matrix mitigates the host foreign body response. J Biomed Mater Res A 2014;102:234-46.
15. Shi L, Ronfard V. Biochemical and biomechanical characterization of porcine small intestinal submucosa (SIS): a mini review. Int J Burns Trauma 2013;3:173-9.

16. Bhol KC, Schechter PJ. Topical nanocrystalline silver cream suppresses inflammatory cytokines and induces apoptosis of inflammatory cells in a murine model of allergic contact dermatitis. Br J Dermatol 2005;152:1235-42.
17. Wood AJ, Cozad MJ, Grant DA, et al. Materials characterization and histological analysis of explanted polypropylene, PTFE, and PET hernia meshes from an individual patient. J Mater Sci Mater Med 2013;24:1113-22.
18. Sistla SC, Reddy R, Dharanipragada K, et al. Enterocutaneous fistula due to mesh fixation in the repair of lateral incisional hernia: a case report. Cases J 2008;1:370.
19. Gómez-Gil V, Rodríguez M, García-Moreno Nisa F, et al. Evaluation of synthetic reticular hybrid meshes designed for intraperitoneal abdominal wall repair: Preclinical and in vitro behavior. PLoS One 2019;14:e0213005.
20. Takeuchi Y, Kurashima Y, Nakanishi Y, et al. Mesh trimming and suture reconstruction for wound dehiscence after huge abdominal intercostal hernia repair: A case report. Int J Surg Case Rep 2018;53:381-5.

Cite this article as: Zhu L, Li H, Chen Y, Dai Y, Li X. Manufacture and evaluation of nano-silver-poly-DL-lactide-co-caprolactone-small intestinal submucosa biological mesh in abdominal wall reconstruction. Ann Transl Med 2024;12(1):4. doi: 10.21037/atm-22-6538